Int. J. Solids Structures Vol. 25, No. 2, pp. 167–188, 1989
Printed in Great Britain.

0020–7683/89 $3.00 + .00

THE SURFACE AND THROUGH CRACK PROBLEMS IN ORTHOTROPIC PLATES

BING-HUA WU and F. ERDOGAN
Department of Mechanical Engineering and Mechanics, Lehigh University, Bethlehem, PA 18015, U.S.A.

(*Received* 26 *March* 1988; *in revised form* 8 *September* 1988)

Abstract—The general mode I crack problem for orthotropic plates under bending and membrane loading is considered. First the bending problem for a series of coplanar through cracks is formulated and the effect of material orthotropy on the stress intensity factors is studied. By varying the six independent material constants one at a time it is shown that, with the exception of Poisson's ratio, all other material constants may have a considerable effect on the stress intensity factors. The surface crack problem is then formulated by using the line spring model with a transverse shear theory of plate bending. Examples are given for composite laminates and crystalline plates containing one or two semielliptic surface cracks and subjected to membrane loading or bending. Here, too, by comparing the results with the isotropic plate solution, it is shown that for severely orthotropic materials such as composite laminates the effect of material orthotropy on the stress intensity factors could be rather significant.

1. INTRODUCTION

In studying the mechanical failure of structural components that may locally be represented by a "plate" or a "shell", very often one has to consider the subcritical crack growth initiating from surface imperfections as a possible mode of failure. The underlying three-dimensional elasticity problem appears to be analytically intractable. Thus, the existing solutions of surface crack problems are based largely on the finite element method (for typical studies see, e.g. Newman and Raju (1979), Raju and Newman (1982), O'Donoghue *et al.* (1986) and Nishioka and Atluri (1982)). Highly effective solutions, however, have also been obtained by using the relatively simple method of a line spring model in conjunction with a plate or a shell theory (Rice and Levy, 1972; Delale and Erdogan, 1982).

In this paper the main interest is in the effect of material orthotropy on the stress intensity factors. In components such as composite laminates, rolled plates and other oriented materials in which the elastic properties in thickness direction may be different from the in-plane values, the assumption of material isotropy may give misleading results. It may be observed that these materials, particularly composites, are multiphase materials and, consequently, in analyzing the processes involving flaws that are of the order of microstructural dimensions, they would have to be treated as non-homogeneous elastic continua. On the other hand if the component contains macroscopic flaws having sizes much greater than the local microstructural dimensions and if the material is sufficiently ordered, it may be treated as a homogeneous anisotropic or orthotropic continuum. In this study it is assumed that the plate is orthotropic and contains coplanar surface cracks that may be longer than the plate thickness. The problem is solved by using the line spring model along with Reissner's plate theory (Reissner, 1945; Medwakowski, 1958). The plate is assumed to be under symmetric bending or membrane loading and only the mode I problem is considered.

2. EQUATIONS OF ORTHOTROPIC PLATES

Following Reissner, if we assume that the stress components σ_{11}, σ_{22} and σ_{12} are linear in the thickness coordinate x_3 and

$$\sigma_{33}(x_1, x_2, h/2) = 0, \quad \sigma_{33}(x_1, x_2, -h/2) = q, \quad \sigma_{3i}(x_1, x_2, \mp h/2) = 0 \quad (i = 1, 2) \quad (1)$$

from the three-dimensional equilibrium equations it may be shown that (Schäfer, 1952; Timoshenko and Woinowsky-Krieger, 1959)

$$\sigma_{11} = \frac{12M_{11}x_3}{h^3}, \quad \sigma_{22} = \frac{12M_{22}x_3}{h^3}, \quad \sigma_{12} = \frac{12M_{12}x_3}{h^3}$$

$$\sigma_{13} = \frac{3V_1}{2h}\left(1 - \frac{4x_3^2}{h^2}\right), \quad \sigma_{23} = \frac{3V_2}{2h}\left(1 - \frac{4x_3^2}{h^2}\right)$$

$$\sigma_{33} = \frac{3q}{4}\left(\frac{2x_3}{h} - \frac{8x_3^3}{3h^3} + \frac{2}{3}\right) \tag{2a-f}$$

where M_{ij} and V_i $(i = 1, 2)$ are, respectively, the moment and transverse shear resultants and h the thickness. Also, from the equilibrium of the plate element we have

$$\sum_1^2 \frac{\partial M_{ij}}{\partial x_j} - V_i = 0 \quad (i = 1, 2), \quad \frac{\partial V_1}{\partial x_1} + \frac{\partial V_2}{\partial x_2} + q = 0. \tag{3a-c}$$

The following average rotations and displacement are now introduced by using the balance of work done by the resultant forces through these average values and by the corresponding stresses σ_{ij} through the actual displacements u_i $(i, j = 1, 2, 3)$ (Schäfer, 1952):

$$\beta_1 = \frac{6}{h^2}\int_{-h/2}^{h/2} u_1 \frac{x_3}{h/2}\,\mathrm{d}x_3$$

$$\beta_2 = \frac{6}{h^2}\int_{-h/2}^{h/2} u_2 \frac{x_3}{h/2}\,\mathrm{d}x_3$$

$$w = \frac{3}{2h}\int_{-h/2}^{h/2} u_3\left(1 - \frac{4x_3^2}{h^2}\right)\mathrm{d}x_3. \tag{4a-c}$$

Let the stress–strain relations of the material be

$$\varepsilon_{ii} = \frac{\partial u_i}{\partial x_i} = \sum_{j=1}^{3} S_{ij}\sigma_{jj} \quad (i = 1, 2, 3)$$

$$2\varepsilon_{23} = \frac{\partial u_2}{\partial x_3} + \frac{\partial u_3}{\partial x_2} = S_{44}\sigma_{23}$$

$$2\varepsilon_{13} = \frac{\partial u_1}{\partial x_3} + \frac{\partial u_3}{\partial x_1} = S_{55}\sigma_{13}$$

$$2\varepsilon_{12} = \frac{\partial u_1}{\partial x_2} + \frac{\partial u_2}{\partial x_1} = S_{66}\sigma_{12}. \tag{5a-f}$$

Note that for orthotropic materials $S_{ij} = S_{ji}$. By integrating in x_3 from eqns (2), (4) and (5) it follows that

$$M_{11} = \frac{h^3}{12(S_{11}S_{22}-S_{12}S_{21})}\left[S_{22}\frac{\partial\beta_1}{\partial x_1} - S_{12}\frac{\partial\beta_2}{\partial x_2} + \frac{6q}{5h}(S_{12}S_{23}-S_{22}S_{13})\right]$$

$$M_{22} = \frac{h^3}{12(S_{11}S_{22}-S_{12}S_{21})}\left[S_{11}\frac{\partial\beta_2}{\partial x_2} - S_{21}\frac{\partial\beta_1}{\partial x_1} + \frac{6q}{5h}(S_{21}S_{13}-S_{23}S_{11})\right]$$

$$M_{12} = \frac{h^3}{12S_{66}}\left(\frac{\partial\beta_1}{\partial x_2} + \frac{\partial\beta_2}{\partial x_1}\right)$$

$$V_1 = \frac{5h}{6S_{55}}\left(\beta_1 + \frac{\partial w}{\partial x_1}\right)$$

$$V_2 = \frac{5h}{6S_{44}}\left(\beta_2 + \frac{\partial w}{\partial x_2}\right). \tag{6a–e}$$

Technically eqns (3) and (6) give the complete formulation of the orthotropic plate under bending. By substituting from eqns (6) into eqns (3) one obtains three second-order equations in β_1, β_2 and w that are equivalent to a sixth-order system. Hence three conditions need to be prescribed on the plate boundaries for a unique solution.

Equations (3) and (6) may also be reduced to the following system in the unknown functions w, V_1 and V_2:

$$V_{1,1} + V_{2,2} = 0$$

$$V_1 + A_1 V_{1,11} + A_2 V_{1,22} - A_3 w_{,111} - A_4 w_{,122} = 0$$

$$V_2 + A_5 V_{2,11} + A_6 V_{2,22} - A_7 w_{,112} - A_8 w_{,222} = 0 \tag{7a–c}$$

where it is assumed that $q = 0$, the standard notation for partial differentiation is used and the constants A_i are

$$A_1 = -\frac{h^2}{10\Delta}\left(S_{22}S_{55} + S_{12}S_{44} - \Delta\frac{S_{44}}{S_{66}}\right), \quad A_2 = -\frac{h^2}{10}\frac{S_{55}}{S_{66}}$$

$$A_3 = -\frac{h^3}{12\Delta}S_{22}, \quad A_4 = A_7 = -\frac{h^3}{12\Delta}\left(\frac{2\Delta}{S_{66}} - S_{12}\right), \quad A_5 = -\frac{h^2}{10S_{66}}S_{44}$$

$$A_6 = -\frac{h^2}{10\Delta}\left(S_{11}S_{44} + S_{12}S_{55} - \Delta\frac{S_{55}}{S_{66}}\right), \quad A_8 = -\frac{h^3}{12\Delta}S_{11}$$

$$\Delta = S_{11}S_{22} - S_{12}S_{21}. \tag{8}$$

By introducing the stress function F such that (Medwakowski, 1958)

$$w = F_{,2} + A_1 F_{,112} + A_2 F_{,222}$$

$$V_1 = A_3 F_{,1112} + A_4 F_{,1222}$$

$$V_2 = -A_3 F_{,1111} - A_4 F_{,1122} \tag{9a–c}$$

eqns (7) may be shown to be identically satisfied provided

$$B_1\frac{\partial^6 F}{\partial x_1^4} + B_2\frac{\partial^4 F}{\partial x_1^2 \partial x_2^2} + B_3\frac{\partial^4 F}{\partial x_2^4} + B_4\frac{\partial^6 F}{\partial x_1^6} + B_5\frac{\partial^6 F}{\partial x_1^4 \partial x_2^2} + B_6\frac{\partial^6 F}{\partial x_1^2 \partial x_2^4} + B_7\frac{\partial^6 F}{\partial x_2^6} = 0 \tag{10}$$

where

$$B_1 = -A_3, \quad B_2 = -2A_4, \quad B_3 = -A_8, \quad B_4 = -A_3A_5, \quad B_7 = -A_2A_8$$
$$B_5 = -A_4A_5 - A_3A_6 - A_1A_4, \quad B_6 = -A_4A_6 - A_2A_4 - A_1A_8. \tag{11}$$

Similarly, with the usual generalized plane stress assumption

$$\sigma_{33} = \sigma_{23} = \sigma_{13} = 0 \tag{12}$$

in terms of the Airy stress function ϕ the membrane problem may be formulated as

$$\frac{\partial^4\phi}{\partial x_1^4} + 2C_1\frac{\partial^4\phi}{\partial x_1^2\partial x_2^2} + C_2^2\frac{\partial^4\phi}{\partial x_2^4} = 0 \tag{13}$$

$$\sigma_{11} = \frac{\partial^2\phi}{\partial x_2^2}, \quad \sigma_{22} = \frac{\partial^2\phi}{\partial x_1^2}, \quad \sigma_{12} = -\frac{\partial^2\phi}{\partial x_1\partial x_2} \tag{14}$$

where

$$C_1 = \frac{S_{12}}{S_{22}} + \frac{S_{66}}{2S_{22}}, \quad C_2 = \left(\frac{S_{11}}{S_{22}}\right)^{1/2}. \tag{15}$$

3. THE THROUGH CRACK PROBLEM—BENDING

Consider now the bending problem for an infinite orthotropic plate containing a series of through cracks on the $x_1 = 0$ plane (Fig. 1). It is assumed that $x_1 = 0$ is a plane of symmetry and through a proper superposition the problem is reduced to a perturbation problem in which self-equilibrating stress resultants acting on the crack surfaces are the only non-zero external loads. By using the standard notation

$$x_1 = x, \quad x_2 = y, \quad x_3 = z, \quad M_{11} = M_{xx}, \ldots, \quad V_1 = V_x, \ldots, \quad \beta_1 = \beta_x, \ldots \tag{16}$$

and by expressing the solution of eqn (10) in terms of the following Fourier integral:

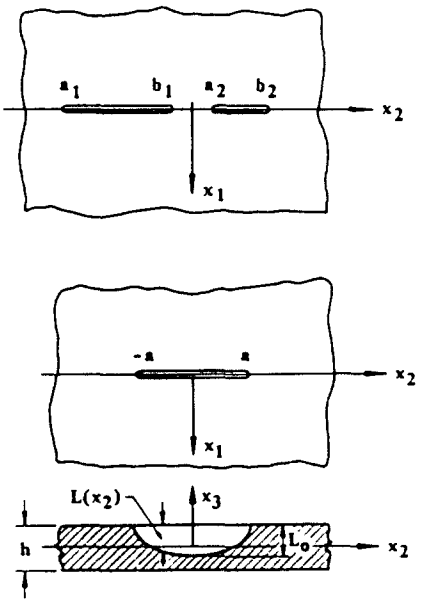

Fig. 1. The geometry of through and surface cracks in a plate.

$$F(x,y)=\frac{1}{2\pi}\int_{-\infty}^{\infty} r(x,\alpha)\,e^{-i\alpha y}\,d\alpha,\quad r(x,\alpha)=R(\alpha)\,e^{mx} \tag{17}$$

the characteristic equation for m is found to be

$$B_4m^6+(B_1-\alpha^2B_5)m^4-(\alpha^2B_2-\alpha^4B_6)m^2+(\alpha^4B_3-\alpha^6B_7)=0. \tag{18}$$

After solving eqn (18) the roots may be ordered such that

$$\mathrm{Re}\,(m_j)<0\quad (j=1,2,3),\quad m_{j+3}=-m_j. \tag{19}$$

Observing the assumed symmetry, it is sufficient to consider $x>0$ half of the plate only. Thus the solution satisfying the regularity condition at $x=\infty$ would be

$$r(x,\alpha)=\sum_{j=1}^{3} R_j(\alpha)\,e^{m_jx}. \tag{20}$$

Note that once the unknown functions R_j $(j=1,2,3)$ are determined, the quantities M_{ij}, V_i and β_i $(i,j=1,2)$ may be obtained from eqns (19), (17), (9) and (6).

The unknown functions R_1, R_2 and R_3 are determined from the following boundary conditions:

$$M_{xy}(0,y)=0,\quad V_x(0,y)=0\quad (-\infty<y<\infty) \tag{21a,b}$$

$$M_{xx}(0,y)=p_1(y),\quad y\in L_c$$
$$\beta_x(0,y)=0,\quad y\in L_c' \tag{22a,b}$$

where p_1 is a known function, L_c refers to the system of cracks on the $x=0$ plane and $(L_c+L_c')=(-\infty,\infty)$.

From eqns (6), (9), (17) and (19) the quantities that appear in boundary conditions (21) and (22) are obtained as

$$M_{xx}(x,y)=\frac{h^3}{12\Delta}\frac{i}{2\pi}\int_{-\infty}^{\infty}\sum_{1}^{3}\theta_{1j}(\alpha)R_j(\alpha)\,e^{m_jx-iy\alpha}\,d\alpha$$

$$M_{xy}(x,y)=\frac{1}{2\pi}\int_{-\infty}^{\infty}\sum_{1}^{3}\theta_{2j}(\alpha)R_j(\alpha)\,e^{m_jx-iy\alpha}\,d\alpha$$

$$V_x(x,y)=\frac{i}{2\pi}\int_{-\infty}^{\infty}\sum_{1}^{3}(A_4\alpha^3m_j-A_3\alpha m_j^3)R_j(\alpha)\,e^{m_jx-iy\alpha}\,d\alpha$$

$$\frac{\partial}{\partial y}\beta_x(x,y)=\frac{1}{2\pi}\int_{-\infty}^{\infty}\sum_{1}^{3}\theta_{3j}(\alpha)R_j(\alpha)\,e^{m_jx-iy\alpha}\,d\alpha\quad (x>0) \tag{23a–d}$$

where Δ is defined by eqn (8) and the functions $\theta_{ij}(\alpha)$ $(i=1,2,3)$ are given in the Appendix. Defining now a new unknown by

$$g(y)=\frac{\partial}{\partial y}\beta_x(0,y)\quad (-\infty<y<\infty) \tag{24}$$

the functions R_j $(j=1,2,3)$ may be obtained in terms of g from eqns (21) and (23b)–(23d). The expressions of R_j thus found are also given in the Appendix.

Condition (22a) which is yet to be satisfied determines the unknown function g. Thus, by substituting from the Appendix and eqn (23a) into eqn (22a) we obtain

$$\lim_{x\to+0}\int_{L_c} g(t)\,dt\int_{-\infty}^{\infty} K(x,\alpha)\,e^{i\alpha(t-y)}\,d\alpha = p_1(y),\quad y\in L_c \tag{25}$$

where K is a known function. The singular behavior of the kernel which determines the asymptotic nature of g near the ends of L_c is obtained by examining K for $\alpha\to\mp\infty$. Let $K^\infty(x,\alpha)$ be the asymptotic form of K for $\alpha\to\mp\infty$. The kernel in eqn (25) may then be expressed as

$$\int_{-\infty}^{\infty} K(x,\alpha)\,e^{i\alpha(t-y)}\,d\alpha = \int_{-\infty}^{\infty} K^\infty(x,\alpha)\,e^{i\alpha(t-y)}\,d\alpha+\int_{-\infty}^{\infty}[K(x,\alpha)-K^\infty(x,\alpha)]\,e^{i\alpha(t-y)}\,d\alpha. \tag{26}$$

After some lengthy manipulations it may be shown that for $x\to 0+$ the first term on the right-hand side of eqn (26) gives a simple Cauchy kernel and the second is bounded. The integral equation, eqn (25), may thus be expressed as

$$\mu_1\int_{L_c}\left[\frac{1}{t-y}+k(y,t)\right]g(t)\,dt = p_1(y),\quad y\in L_c \tag{27}$$

where μ_1 is a material constant and the Fredholm kernel is obtained from

$$k(y,t) = \int_{-\infty}^{\infty}[K(0,\alpha)-K^\infty(0,\alpha)]\,e^{i\alpha(t-y)}\,d\alpha. \tag{28}$$

Note that if L_c consists of the line segments L_i $(i=1,\ldots,n)$ on the y-axis, from eqn (24) it follows that eqn (25) must be solved under the following single-valuedness conditions:

$$\int_{L_i} g(y)\,dy = 0\quad (i=1,\ldots,n). \tag{29}$$

For coplanar through cracks along $L_c=\sum_1^n L_i$, $L_i=(a_i,b_i)$, the simplest way of solving eqn (27) would be to let

$$g(y)=g_i(y),\quad p_1(y)=p_{1i}(y),\quad a_i<y<b_i\quad (i=1,\ldots,n) \tag{30}$$

rewrite eqns (27) and (29) as

$$\mu_1\sum_{j=1}^{n}\int_{a_j}^{b_j}\left[\frac{1}{t-y}+k(y,t)\right]g_j(t)\,dt = p_{1i}(y),\quad a_i<y<b_i\quad (i=1,\ldots,n) \tag{31}$$

$$\int_{a_i}^{b_i} g_i(y)\,dy = 0\quad (i=1,\ldots,n) \tag{32}$$

and treat eqn (29) as a system of singular integral equations in $g_1,\ldots,g_n$. The intervals (a_i,b_i) may then be separately normalized to $(-1,1)$ and the system may be solved by using a standard Gauss–Chebyshev integration technique (Erdogan, 1978). Referring to, e.g. Muskhelishvili (1953), it is known that the solution of eqn (31) is of the form

$$g_i(y) = \frac{G_i(y)}{[(b_i-y)(y-a_i)]^{1/2}}, \quad a_i < y < b_i \quad (i = 1, \ldots, n) \tag{33}$$

where the functions G_i are bounded in the closed interval $[a_i, b_i]$ and $G_i(a_i) \neq 0$, $G_i(b_i) \neq 0$ $(i = 1, \ldots, n)$.

In this study the primary interest is in the stress intensity factors at the crack ends a_i and b_i $(i = 1, \ldots, n)$. The standard definition of the mode I stress intensity factor at, e.g. $y = b_i$ is

$$k_1(b_i) = \lim_{y \to b_i + 0} \sqrt{(2(y-b_i))}\sigma_{xx}(0, y, z). \tag{34}$$

From eqns (22) and the derivation of the integral equation, eqn (27), we observe that the left-hand side of eqn (27) or (31) corresponds to $M_{xx}(0, y)$ for y outside as well as inside the cracks. Thus, from the asymptotic analysis of the solution of the singular integral equations, eqn (31), near the end points a_i and b_i it may be shown that

$$\lim_{y \to b_i + 0} \sqrt{(2(y-b_i))}M_{xx}(0, y) = -\lim_{y \to b_i - 0} \sqrt{(2(b_i-y))}\pi\mu_1 g_i(y)$$

$$\lim_{y \to a_i - 0} \sqrt{(2(a_i-y))}M_{xx}(0, y) = \lim_{y \to a_i + 0} \sqrt{(2(y-a_i))}\pi\mu_1 g_i(y) \quad (i = 1, \ldots, n). \tag{35a, b}$$

From eqns (2a) and (33)–(35) it then follows that

$$k_1(b_i, z) = -\pi\mu_1 \frac{12z}{h^3} \lim_{y \to b_i - 0} \sqrt{(2(b_i-y))}g_i(y)$$

$$= -\pi\mu_1 \frac{12z}{h^3} \frac{G_i(b_i)}{\sqrt{((b_i-a_i)/2)}}$$

$$k_1(a_i, z) = \pi\mu_1 \frac{12z}{h^3} \frac{G_i(a_i)}{\sqrt{((b_i-a_i)/2)}} \quad (i = 1, \ldots, n). \tag{36a, b}$$

4. THE THROUGH CRACK PROBLEM—MEMBRANE LOADING

For the in-plane loading problem expressing the solution of eqn (13) by

$$\phi(x, y) = \frac{1}{2\pi} \int_{-\infty}^{\infty} \psi(x, \alpha)\, e^{-i\alpha y}\, d\alpha, \quad \psi = P(\alpha)\, e^{nx} \tag{37}$$

the characteristic equation is found to be

$$\left(\frac{n}{\alpha}\right)^4 + 2C_1\left(\frac{n}{\alpha}\right)^2 + C_2^2 = 0 \tag{38}$$

where C_1 and C_2 are given by eqns (15). Noting that since generally $S_{12} < 0$, the roots of eqn (38) may be real or complex. Thus, the solution of eqns (37) satisfying the regularity conditions at $x = \infty$ may be expressed as

$$\psi(x, \alpha) = \sum_1^2 P_j(\alpha)\, e^{-n_j x|\alpha|} \tag{39}$$

if the roots $(n/\alpha) = \mp n_i$ $(i = 1, 2)$ are real (defined as "material type I"), and

$$\psi(x,\alpha) = [P_1(\alpha)\cos q_2\alpha x + P_2(\alpha)\sin q_2\alpha x]\,e^{-q_1|\alpha x|} \tag{40}$$

if the roots $(n\ \alpha) = \mp(q_1 \mp iq_2)$ are complex (defined as "material type 2") where n_1, n_2, q_1 and q_2 are positive constants. The unknown functions P_1 and P_2 are determined from the following boundary conditions:

$$N_{xy}(0,y) = 0, \quad -\infty < y < \infty \tag{41}$$

$$\left.\begin{aligned} N_{xx}(0,y) &= p_2(y), \quad y \in L \\ u_x(0,y) &= 0, \quad y \in L'. \end{aligned}\right\} \tag{42a, b}$$

Defining

$$\frac{\partial}{\partial y}u_x(0,y) = f(y), \quad -\infty < y < \infty \tag{43}$$

and following a procedure similar to that described in the previous section, the integral equation to determine $f(y)$ is found to be

$$\mu_2 \int_{L_c} \frac{f(t)}{t-x}\,dt = p_2(y), \quad y \in L_c, \quad L_c = \sum_1^n L_i \tag{44}$$

where

$$\mu_2 = \frac{h}{\pi} \frac{1}{S_{22}n_1n_2(n_1+n_2)} \tag{45}$$

for material type 1, and

$$\mu_2 = \frac{h}{\pi} \frac{1}{2S_{22}q_1(q_1^2+q_2^2)} \tag{46}$$

for material type 2. Again, from eqns (42b) and (43) it follows that f must satisfy the following single valuedness conditions:

$$\int_{L_i} f(t)\,dt = 0 \quad (i = 1,2,\ldots,n). \tag{47}$$

Also, if we let

$$f(y) = f_i(y) = \frac{F_i(y)}{[(b_i-y)(y-a_i)]^{1/2}}, \quad a_i < y < b_i \quad (i = 1,\ldots,n) \tag{48}$$

and observe that $p_2(y) = h\sigma_{xx}(0,y)$ the stress intensity factors at the crack tips b_i and a_i are found to be (see eqn (34))

$$\left.\begin{aligned} k_1(b_i) &= -\frac{\pi\mu_2}{h}\frac{F_i(b_i)}{\sqrt{((b_i-a_i)/2)}} \\ k_1(a_i) &= \frac{\pi\mu_2}{h}\frac{F_i(a_i)}{\sqrt{((b_i-a_i)/2)}} \end{aligned}\right\} \quad (i = 1,\ldots,n). \tag{49a, b}$$

5. THE SURFACE CRACK PROBLEM

In the case of a plate containing a series of coplanar through cracks the bending and membrane problems are uncoupled and the respective solutions are given in the previous

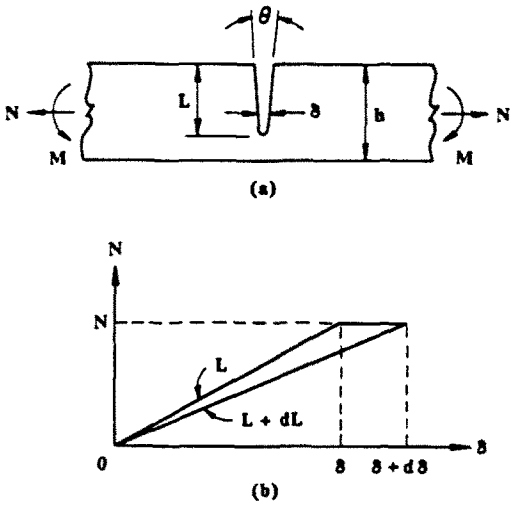

Fig. 2. The edge-cracked strip under plane strain conditions used in the development of the line spring model.

sections. In plates with surface cracks, since $z = 0$ is no longer a plane of symmetry (as in membrane loading) or antisymmetry (as in bending), clearly the problem cannot be uncoupled. In a plate with surface cracks the net ligament under the crack would generally have a constraining effect on the opening of the crack surfaces. In this case, representing the net ligament stress $\sigma_{xx}(0, y, z)$, $(a_i < y < b_i, -h/2 < z < h/2 - L$, Fig. 2) by a membrane load N and a bending moment M, and the crack surface displacement due to N and M as an opening (at $z = 0$) δ and a rotation θ, the three-dimensional crack problem may be reduced to a two-dimensional coupled bending/membrane plate problem. Furthermore, by assuming that the relationship between (N, M) and (δ, θ) may be found from the plane strain solution of an edge-cracked strip, the pair of functions (δ, θ) or (N, M) can be determined from the corresponding mixed boundary value problem for a plate having through cracks in which N and M are treated as unknown crack surface loads.

We now observe that in the absence of any cracks if the applied loads at the $x = 0$ plane are given by

$$M_{xx}(0, y) = M_0(y), \quad M_{xy}(0, y) = 0, \quad V_x(0, y) = 0 \tag{50}$$

$$N_{xx}(0, y) = N_0(y), \quad N_{xy}(0, y) = 0 \tag{51}$$

the surface crack problem may be formulated by using the through crack solution in which the (unknown) crack surface tractions include $M(y)$ and $N(y)$ representing the effect of net ligament stress σ_{xx}. Thus, the integral equations, eqns (27) and (44), may be modified as follows:

$$\mu_1 \int_L \left[\frac{1}{t-y} + k(y, t)\right] g(t)\, dt = -M_0(y) + M(y), \quad y \in L \tag{52}$$

$$\mu_2 \int_L \frac{f(t)}{t-x}\, dt = -N_0(y) + N(y), \quad y \in L. \tag{53}$$

In order to solve these equations first the relationship between the pair of functions (M, N) and (θ, δ) must be established, where

$$\theta(y) = 2\beta_x(y), \qquad g(y) = \frac{1}{2}\frac{d\theta}{dy}$$

$$\delta(y) = 2u_x(0, y), \quad f(y) = \frac{1}{2}\frac{d\delta}{dy}. \tag{54a–d}$$

This relationship may be found by expressing the energy available for fracture in two different ways: as the strain energy release rate in terms of the stress intensity factor and as the product of the load–load point displacement at the $x_3 = 0$ plane (Rice and Levy, 1972). In an orthotropic plate with an edge crack subjected to a membrane load N and a bending moment M (Fig. 2(a)), if k_1 is the stress intensity factor obtained from the plane strain solution then, from the incremental crack closure, the rate of energy available for fracture may be obtained as

$$\mathcal{G} = \frac{\partial}{\partial L}(U - V) = \frac{\pi}{\mu_3}k_1^2 \tag{55}$$

where U is the work done by the applied loads, V the strain energy, and μ_3 a material constant given by the elasticity matrix S_{ij} as follows (Sih and Liebowitz, 1968):

$$\mu_3 = \frac{\sqrt{2}}{\sqrt{(b_{11}b_{22})}}\left(\left(\frac{b_{22}}{b_{11}}\right)^{1/2} + \frac{2b_{12} + b_{66}}{2b_{11}}\right)^{-1/2} \tag{56}$$

$$b_{11} = (S_{11}S_{22} - S_{23}^2)/S_{22}, \quad b_{22} = (S_{11}S_{22} - S_{12}^2)/S_{22}$$

$$b_{12} = S_{55}, \quad b_{66} = (S_{11}S_{22} - S_{12}S_{21})/S_{22}. \tag{57}$$

For the edge crack shown in Fig. 2(a) the stress intensity factor may be expressed as

$$k_1(s) = \sqrt{h}[\sigma_t g_t(s) + \sigma_b g_b(s)], \quad s(y) = L(y)/h \tag{58}$$

$$\sigma_t = N/h, \quad \sigma_b = 6M/h^2 \tag{59}$$

where the "shape functions" g_t and g_b are obtained from the results given in Kaya and Erdogan (1980). Referring to Fig. 2(b), the energy available for fracture may also be written as (Erdogan, 1986)

$$dU = N\,d\delta + M\,d\theta, \quad dV = \tfrac{1}{2}(N\,d\delta + M\,d\theta) \tag{60}$$

$$\mathcal{G} = \frac{\partial}{\partial L}(U - V) = \frac{1}{2}\left(N\frac{\partial \delta}{\partial L} + M\frac{\partial \theta}{\partial L}\right). \tag{61}$$

From eqns (55), (58) and (61) it may be shown that

$$\frac{h}{6}\theta = \frac{2h}{\mu_3}(\alpha_{bb}\sigma_b + \alpha_{bt}\sigma_t)$$

$$\delta = \frac{2h}{\mu_3}(\alpha_{tb}\sigma_b + \alpha_{tt}\sigma_t) \tag{62a, b}$$

where the compliance coefficients α_{ij} are given by

$$\alpha_{ij} = \frac{2h}{\mu_3}\int_0^L g_i g_j\,dL \quad (i, j = b, t). \tag{63}$$

Referring now to eqns (54) we have

$$\theta(y) = 2\int_{a_i}^{y} g(t)\,dt, \quad \delta(y) = 2\int_{a_i}^{y} f(t)\,dt, \quad y \in L_i. \tag{64a, b}$$

Thus, by substituting from eqns (59), (62) and (64) into eqns (52) and (53) we obtain

$$\mu_1 \sum_{j=1}^{n} \int_{a_j}^{b_j} \left[\frac{1}{t-y} + k(y,t)\right] g_j(t)\,dt - \mu_3 \left[\frac{h^2}{36}\gamma_{bb}\int_{a_i}^{y} g_i(t)\,dt + \frac{h}{6}\gamma_{bt}\int_{a_i}^{y} f_i(t)\,dt\right]$$
$$= -M_0(y), \quad a_i < y < b_i$$

$$\mu_2 \sum_{j=1}^{n} \int_{a_j}^{b_j} \frac{f_j(t)}{t-y}\,dt - \mu_3 \left[\frac{h}{6}\gamma_{tb}\int_{a_i}^{y} g_i(t)\,dt + \gamma_{tt}\int_{a_i}^{y} f_i(t)\,dt\right]$$
$$= -N_0(y), \quad a_i < y < b_i \quad (i = 1, \ldots, n) \tag{65a, b}$$

where γ_{ij} $(i, j = \mathrm{b}, \mathrm{t})$ are functions of y and are given by

$$\gamma_{bb} = \frac{\alpha_{tt}}{\Delta_0}, \quad \gamma_{bt} = -\frac{\alpha_{bt}}{\Delta_0}, \quad \gamma_{tb} = -\frac{\alpha_{tb}}{\Delta_0}, \quad \gamma_{tt} = \frac{\alpha_{bb}}{\Delta_0}$$
$$\Delta_0 = \alpha_{bb}\alpha_{tt} - \alpha_{bt}\alpha_{tb}. \tag{66}$$

The shape functions g_t and g_b are tabulated in Kaya and Erdogan (1980). To simplify the manipulations they are represented here in the following analytical form:

$$g_t(s) = \sqrt{s}\sum_{0}^{K} c_k s^{2k}, \quad s = L/h$$
$$g_b(s) = \sqrt{s}\sum_{0}^{K} d_k s^{2k}, \quad s = L/h. \tag{67a, b}$$

For materials 1–3 the stress intensity factors obtained from the plane strain solution of a strip with an edge crack under a membrane load N or a bending moment M are given in Table 3 (Fig. 2(a)). Table 4 shows the corresponding coefficients c_k and d_k giving the shape functions g_t and g_b defined by eqns (58) and (67). After solving the integral equations, eqns (65), for g and f, the stress intensity factor for the ith crack may be obtained by substituting from

$$\sigma_b(y) = \frac{\mu_3}{6}\gamma_{bb}(y)\int_{a_i}^{y} g\,dt + \frac{\mu_3}{h}\gamma_{bt}(y)\int_{a_i}^{y} f\,dt \quad (a_i < y < b_i)$$
$$\sigma_t(y) = \frac{\mu_3}{6}\gamma_{tb}(y)\int_{a_i}^{y} g\,dt + \frac{\mu_3}{h}\gamma_{tt}(y)\int_{a_i}^{y} f\,dt \quad (a_i < y < b_i) \quad (i = 1, \ldots, n) \tag{68a, b}$$

into eqns (58).

6. RESULTS

The elastic properties of the materials considered in the examples are given in Table 1. Material 1 is basically isotropic and is included for the purpose of comparing the results with previous studies. Materials 2 and 3 are graphite-epoxy composite laminates. Except for the 90° rotation in the axes of orthotropy, these two materials are identical. Some limited results are also obtained for a crystalline material, TOPAZ ($SiO_2Al_2(FOH)_2$) (Hearmon, 1961). Table 2 shows the properties of TOPAZ designated as materials 4 and 5. Again, the difference between these two materials is a 90° rotation in axes of orthotropy. In all cases the crack is located in the $x_1 = x = 0$ plane.

Table 1. Elastic constants of materials 1–3

		Material 1	Material 2	Material 3
E_x	psi	2.2447×10^6	5.86×10^6	22.2×10^6
	GPa	15.477	40.405	153.069
E_y	psi	2.26×10^6	22.2×10^6	5.86×10^6
	GPa	15.583	153.069	40.405
E_z	psi	2.26×10^6	3.3×10^6	3.3×10^6
	GPa	15.583	22.754	22.754
G_{xy}	psi	0.866×10^6	4.25×10^6	4.25×10^6
	GPa	5.971	29.304	29.304
G_{yz}	psi	0.866×10^6	0.592×10^6	0.225×10^6
	GPa	5.971	4.082	1.551
G_{xz}	psi	0.866×10^6	0.255×10^6	0.592×10^6
	GPa	5.971	1.551	4.082
ν_{xy}		0.3	0.484	1.834
ν_{yz}		0.3	0.195	0.261
ν_{xz}		0.3	0.261	0.195

Table 2. Elastic constants of TOPAZ, materials 4 and 5 (in units of 10^{-13} cm^2 dyn^{-1} (Hearmon, 1961))

Material 4	$S_{11} = 4.43$	$S_{22} = 3.53$	$S_{33} = 3.84$
	$S_{12} = -1.38$	$S_{13} = -0.86$	$S_{23} = -0.66$
	$S_{44} = 9.25$	$S_{55} = 7.52$	$S_{66} = 7.63$
Material 5	$S_{11} = 3.53$	$S_{22} = 4.43$	$S_{33} = 3.84$
	$S_{12} = -1.38$	$S_{13} = -0.66$	$S_{23} = -0.86$
	$S_{44} = 7.52$	$S_{55} = 9.25$	$S_{66} = 7.63$

Table 3. Stress intensity factors in a strip containing an edge crack under membrane loading N and bending moment M ($\sigma_t = N/h$, $\sigma_b = 6M/h^2$ (Fig. 2(a))

	Material 1		Material 2		Material 3	
$\frac{L}{h}$	$\frac{k_t}{\sigma_t\sqrt{L}}$	$\frac{k_b}{\sigma_b\sqrt{L}}$	$\frac{k_t}{\sigma_t\sqrt{L}}$	$\frac{k_b}{\sigma_b\sqrt{L}}$	$\frac{k_t}{\sigma_t\sqrt{L}}$	$\frac{k_b}{\sigma_b\sqrt{L}}$
0.001	1.122	1.120	1.042	1.041	1.050	1.049
0.1	1.189	1.047	1.129	0.992	1.134	0.996
0.2	1.367	1.055	1.318	1.013	1.321	1.016
0.3	1.660	1.124	1.607	1.083	1.611	1.086
0.4	2.111	1.261	2.042	1.211	2.048	1.215
0.5	2.825	1.498	2.721	1.430	2.730	1.436
0.6	4.033	1.915	3.860	1.814	3.876	1.823
0.7	6.355	2.728	6.038	2.563	6.068	2.577
0.8	11.955	4.691	11.277	4.372	11.350	4.402

Table 4. The coefficients c_k and d_k for the shape functions g_t and g_b (eqn (67))

	Material 1		Material 2		Material 3	
k	c_k	d_k	c_k	d_k	c_k	d_k
0	1.122	1.120	1.047	1.043	1.055	1.051
1	6.520	−1.887	7.639	−1.610	7.461	−1.664
2	−12.388	18.014	−27.969	17.276	−25.426	17.517
3	89.055	−87.385	175.360	−84.989	160.659	−85.711
4	−188.608	241.912	−439.451	232.556	−396.808	234.182
5	207.387	−319.940	557.540	−304.196	498.577	−306.252
6	−32.052	168.011	−222.80	158.307	−191.359	159.403

Table 5. The effect of Poisson's ratio and crack length on the normalized stress intensity factor $k_1/\sigma_b\sqrt{a}$ in an isotropic plate containing a through crack and subjected to bending $M_{xx}^c = M_0$: $\sigma_b = 6M_0/h^2$ (Fig. 1, eqn (71))

	ν		
a/h	0.5	0.3	0
0.01	0.9995	0.9993	0.9990
0.05	0.9900	0.9885	0.9851
0.1	0.9717	0.9676	0.9583
0.25	0.9111	0.8992	0.8735
0.5	0.8383	0.8193	0.7804
1	0.7707	0.7475	0.7020
2	0.7247	0.6997	0.6518
4	0.6960	0.6701	0.6211
6	0.6847	0.6586	0.6091
10	0.6746	0.6481	0.5984
100	0.6575	0.6306	0.5803
200		0.6292	
1000		0.6276	

By using the solution given in this paper, first the results given by Joseph and Erdogan (1987) for an isotropic plate with a through crack under bending are reproduced. These results are given in Table 5 for reference. The stress intensity factors shown in Table 5 are obtained from eqns (32) and (36) for a single crack of length $2a$ and for the uniform bending moment (see eqn (21) and Fig. 1)

$$M_{xx}(0, y) = p_1(y) = -M_0, \quad -a < y < a. \tag{69}$$

In terms of the surface stress given by

$$\sigma_b = \frac{6M_0}{h^2} \tag{70}$$

for a single crack the stress intensity factor defined by eqn (36) may be normalized and written as follows:

$$\frac{k_1(a, z)}{\sigma_b\sqrt{a}} = \frac{z}{h/2}\frac{k_1(a)}{\sigma_b\sqrt{a}}. \tag{71}$$

The notation

$$k_1(b_i, h/2) = k_1(b_i), \quad k_1(a_i, h/2) = k_1(a_i) \quad (i = 1, \ldots, n) \tag{72}$$

is used in all through crack results given in this paper.

The effect of material orthotropy on the stress intensity factor in a plate containing a single through crack under uniform bending is shown in Fig. 3 where material 1 is isotropic and the properties of materials 2 and 3 are given in Table 1. The figure shows that the deviation from isotropic results can be considerable. It should be emphasized that in the particular plate theory used full material orthotropy had to be considered. Hence, from the results given in Section 2 it may be seen that with $S_{ij} = S_{ji}$ there are eight independent material constants in bending† and four in membrane formulation of the plate. Furthermore, by normalizing, the number of independent material parameters can always be reduced by one. From eqns (13)–(15) it may also be observed that for $q = 0$ the bending formulation is not dependent on S_{13} and S_{23} (or ν_{13} and ν_{23}), and consequently in the through crack case there are only six independent constants. However, in formulating the

† S_{33} does not enter into the formulation.

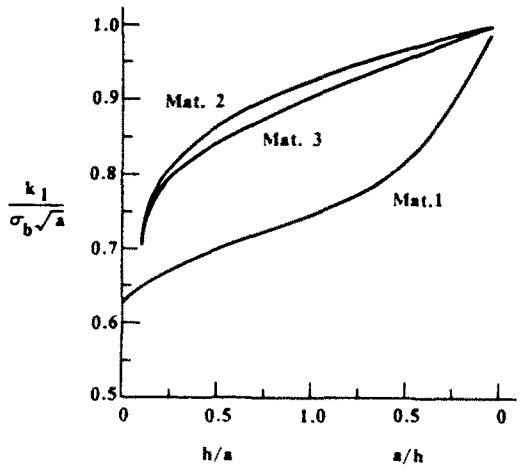

Fig. 3. The effect of the plate thickness on the normalized stress intensity factor in a plate containing a single through crack under bending moment $M_x' = M_0$, $\sigma_b = 6M_0/h^2$ (Fig. 1, Table 1).

part-through crack problem, in addition to membrane loading and bending of the plate, one has to consider the plane strain crack problem for the orthotropic medium in the x–z plane. As a result, the formulation of the surface crack problem involves all nine material constants.

In an attempt to determine the effect of the individual material constants, the through crack bending stress intensity factors for $a/h = 1$ were calculated for a series of fictitious orthotropic plates where in each case only one or two material constants are varied. The results are shown in Fig. 4. The stress intensity factors given in Fig. 4 are calculated for $\nu_{12} = 0.5$. In these problems the effect of Poisson's ratio is not very significant and is quite similar to that observed for isotropic plates (Table 5). A sample result showing the effect of G_{13} and ν_{12} is also given in Table 6. With the exception of the particular material constant that was varied, the plate is assumed to be "isotropic". For example in Table 6 the material

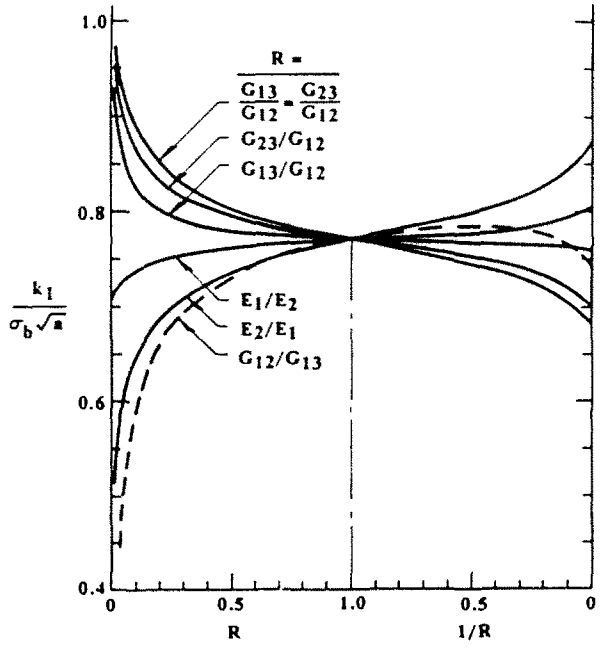

Fig. 4. The effect of individual material constants on the normalized stress intensity factor in a plate containing a single through crack under bending moment $M_x' = M_0$, $\sigma_b = 6M_0/h^2$, $(a/h) = 1$.

Table 6. The effect of the transverse shear modulus G_{13} on the normalized stress intensity factor $k_1/\sigma_b\sqrt{a}$ in an orthotropic plate with a through crack under bending $M_{xx}^{\infty} = M_0, \sigma_b = 6M_0/h^2, a/h = 1$ (Fig. 1, eqn (71))

$\frac{G_{13}}{G_{12}}$	ν_{12} 0.5	0
0.001	0.985	0.978
0.01	0.930	0.899
0.1	0.826	0.765
0.2	0.801	0.736
0.5	0.780	0.713
1	0.771	0.702
2	0.766	0.697
5	0.763	0.694
10	0.762	0.692
100	0.7605	0.6911
1000	0.7604	0.6910
10,000	0.7604	0.6910

Table 7. The effect of the interaction of two coplanar through cracks on the normalized stress intensity factors in an isotropic plate under bending $M_{xx}^{\infty} = M_0, \sigma_b = 6M_0/h^2, \nu = 0.3, a = (b_1-a_1)/2, c = (b_2-a_2)/2, d = a_2-b_1$ (Fig. 1, eqn (71))

	$\frac{c}{a}$	$\frac{d}{a} \to 0.1$	0.25	0.5	1	2	∞
$\frac{k_1(a_1)}{\sigma_b\sqrt{a}}$	1	0.8799	0.8551	0.8313	0.8045	0.7798	0.7475
	0.5	0.8071	0.7938	0.7821	0.7698	0.7593	0.7475
	0.25	0.7711	0.7647	0.7598	0.7551	0.7513	0.7475
	0.1	0.7532	0.7512	0.7500	0.7490	0.7482	0.7475
$\frac{k_1(b_1)}{\sigma_b\sqrt{a}}$	1	1.294	1.076	0.9599	0.8697	0.8049	0.7475
	0.5	1.063	0.9143	0.8458	0.7995	0.7698	0.7475
	0.25	0.9161	0.8220	0.7863	0.7663	0.7550	0.7475
	0.1	0.8088	0.7678	0.7563	0.7514	0.7489	0.7475
$\frac{k_1(a_2)}{\sigma_b\sqrt{a}}$	1	1.294	1.076	0.9599	0.8697	0.8049	0.7475
	0.5	1.012	0.8405	0.7498	0.6786	0.6261	0.5794
	0.25	0.7990	0.6595	0.5867	0.5297	0.4872	0.4496
	0.1	0.5647	0.4577	0.4037	0.3627	0.3325	0.3060
$\frac{k_1(b_2)}{\sigma_b\sqrt{a}}$	1	0.8799	0.8551	0.8313	0.8045	0.7798	0.7475
	0.5	0.7395	0.7071	0.6771	0.6434	0.6132	0.5794
	0.25	0.6275	0.5867	0.5507	0.5135	0.4816	0.4496
	0.1	0.4817	0.4293	0.3917	0.3577	0.3308	0.3060

constants are assumed to be $E_{11} = E_{22}, G_{12} = G_{23} = E_{11}/2(1+\nu_{12})$ and G_{13} is varied relative to the remaining constants. As the varying material constant approaches infinity, there does not seem to be any difficulty in calculating the limiting value of the stress intensity factor (see Table 6 and Fig. 4). This is only partly the case for $R \to 0$. One of the interesting results observed here was that as G_{13}, G_{23} or both approach zero, the stress intensity factor tends to the plane stress value $\sigma_b\sqrt{a}$. In all cases k_1 is a monotonically increasing or decreasing function of R except for varying G_{12} for which k_1 seems to have a maximum at $R \cong 0.75$.

To give an example for the interaction of coplanar through cracks the problem of two cracks shown in Fig. 1 is considered. The stress intensity factors for the bending problem for an isotropic plate (reproducing the results given by Joseph and Erdogan (1987) as the special case) are shown in Table 7. The corresponding results for the orthotropic plates are shown in Tables 8 and 9 (see Table 1 for material constants). For comparison Table 10 gives the stress intensity factors for through cracks in a plate under membrane loading for which the results for isotropic and orthotropic materials are, of course, identical.† The contents of these tables are self-explanatory and such trends as the stress intensity factors

† This result follows directly from eqn (44), see also Krenk (1975).

Table 8. The effect of the interaction of two coplanar through cracks on the normalized stress intensity factors in an orthotropic plate under bending $M_{xx}^{\infty} = M_0$, $\sigma_b = 6M_0/h^2$, $a = (b_1 - a_1)/2$, $c = (b_2 - a_2)/2$, $d = a_2 - b_1$ (Fig. 1, eqn (71)), material 2

	$\frac{c}{a}$	$\frac{d}{a} \to 0.1$	0.25	0.5	1	2	∞
$\frac{k_1(a_1)}{\sigma_b\sqrt{a}}$	1	1.051	1.023	1.001	0.9782	0.9590	0.9276
	0.5	0.9814	0.9658	0.9546	0.9451	0.9373	0.9276
	0.25	0.9488	0.9411	0.9363	0.9328	0.9305	0.9276
	0.1	0.9329	0.9305	0.9293	0.9285	0.9280	0.9276
$\frac{k_1(b_1)}{\sigma_b\sqrt{a}}$	1	1.591	1.274	1.122	1.029	0.9773	0.9276
	0.5	1.320	1.106	1.015	0.9665	0.9441	0.9276
	0.25	1.137	1.008	0.9614	0.9405	0.9325	0.9276
	0.1	1.003	0.9500	0.9353	0.9301	0.9284	0.9276
$\frac{k_1(a_2)}{\sigma_b\sqrt{a}}$	1	1.591	1.274	1.122	1.029	0.9773	0.9276
	0.5	1.221	0.9665	0.8424	0.7658	0.7240	0.6851
	0.25	0.9261	0.7202	0.6188	0.5567	0.5236	0.4943
	0.1	0.6327	0.4774	0.4023	0.3577	0.3348	0.3154
$\frac{k_1(b_2)}{\sigma_b\sqrt{a}}$	1	1.051	1.023	1.001	0.9782	0.9590	0.9276
	0.5	0.8441	0.8019	0.7687	0.7386	0.7151	0.6851
	0.25	0.6817	0.6228	0.5790	0.5436	0.5201	0.4943
	0.1	0.5143	0.4375	0.3880	0.3535	0.3335	0.3154

Table 9. The effect of the interaction of two coplanar through cracks on the normalized stress intensity factors in an orthotropic plate under bending $M_{xx}^{\infty} = M_0$, $\sigma_b = 6M_0/h^2$, $a = (b_1 - a_1)/2$, $c = (b_2 - a_2)/2$, $d = a_2 - b_1$ (Fig. 1, eqn (71)), material 3

	$\frac{c}{a}$	$\frac{d}{a} \to 0.1$	0.25	0.5	1	2	∞
$\frac{k_1(a_1)}{\sigma_b\sqrt{a}}$	1	1.031	1.004	0.9821	0.9582	0.9375	0.9050
	0.5	0.9595	0.9442	0.9332	0.9238	0.9152	0.9050
	0.25	0.9263	0.9188	0.9141	0.9106	0.9083	0.9050
	0.1	0.9194	0.9080	0.9068	0.9060	0.9059	0.9050
$\frac{k_1(b_1)}{\sigma_b\sqrt{a}}$	1	1.547	1.246	1.101	1.011	0.9581	0.9050
	0.5	1.287	1.080	0.9917	0.9452	0.9228	0.9050
	0.25	1.111	0.9841	0.9385	0.9183	0.9103	0.9050
	0.1	0.9103	0.9271	0.9127	0.9076	0.9054	0.9050
$\frac{k_1(a_2)}{\sigma_b\sqrt{a}}$	1	1.547	1.246	1.101	1.011	0.9581	0.9050
	0.5	1.206	0.9550	0.8301	0.7507	0.7067	0.6752
	0.25	0.9205	0.7171	0.6150	0.5505	0.5154	0.4912
	0.1	0.6308	0.4775	0.4019	0.3555	0.3311	0.3149
$\frac{k_1(b_2)}{\sigma_b\sqrt{a}}$	1	1.031	1.004	0.9821	0.9582	0.9375	0.9050
	0.5	0.8289	0.7869	0.7529	0.7216	0.6981	0.6752
	0.25	0.6777	0.6187	0.5736	0.5364	0.5116	0.4912
	0.1	0.5140	0.4375	0.3872	0.3510	0.3300	0.3149

tending to the corresponding single crack values as $d \to \infty$, and $k_1(b_1)$ and $k_1(a_2)$ becoming unbounded as $d \to 0$ are the expected results.

Some results for a single semielliptic surface crack in an orthotropic plate under a bending moment $M_{xx}^{\infty} = M_0$ and a membrane load $N_{xx}^{\infty} = N_0$ (Fig. 1) are given in Figs 5–8. The normalizing stress intensity factors k_b^{∞} and k_t^{∞} in these and in the remaining surface crack examples are the corresponding plane strain values obtained from a strip with an edge crack of length L_0 subjected to bending or tension and are given in Table 3 (where $L = L_0$, $\sigma_b = 6M_0/h^2$, $\sigma_t = N_0/h$). The profile of the crack is

$$L(y) = L_0\sqrt{(1-(y/a)^2)}. \tag{73}$$

Figures 5 and 6 show the normalized stress intensity factors at $x_2 = y = 0$ (Fig. 1) for the plate under bending and tension, respectively. Note that for $(a/h) \to \infty$, $k_b \to k_b^{\infty}$ and $k_t \to k_t^{\infty}$, that is the plane strain results are recovered. For $a/h = 1$ the distribution of the

Table 10. The effect of crack interaction on the normalized stress intensity factors in an isotropic or orthotropic plate under uniform tension $N_{xx} = N_0$, $\sigma_t = N_0/h$, $a = (b_1 - a_1)/2$, $c = (b_2 - a_2)/2$, $d = a_2 - b_1$ (Fig. 1)

	$\frac{c}{a}$	$\frac{d}{a} \to 0.1$	0.25	0.5	1	2	∞
$\frac{k_1(a_1)}{\sigma_t\sqrt{a}}$	1	1.151	1.112	1.0811	1.052	1.028	1.000
	0.5	1.066	1.045	1.030	1.018	1.009	1.000
	0.25	1.026	1.016	1.010	1.005	1.003	1.000
	0.1	1.007	1.004	1.002	1.001	1.000	1.000
$\frac{k_1(b_1)}{\sigma_t\sqrt{a}}$	1	1.795	1.414	1.229	1.113	1.048	1.000
	0.5	1.449	1.206	1.100	1.043	1.016	1.000
	0.25	1.234	1.090	1.038	1.014	1.005	1.000
	0.1	1.083	1.025	1.009	1.003	1.001	1.000
$\frac{k_1(a_2)}{\sigma_t\sqrt{a}}$	1	1.795	1.414	1.229	1.113	1.048	1.000
	0.5	1.329	1.035	0.8889	0.7962	0.7446	0.7071
	0.25	0.9915	0.7595	0.5955	0.5683	0.5280	0.5000
	0.1	0.6732	0.5006	0.4151	0.3624	0.3349	0.3162
$\frac{k_1(b_2)}{\sigma_t\sqrt{a}}$	1	1.151	1.112	1.0811	1.052	1.028	1.000
	0.5	0.8956	0.8429	0.8007	0.7626	0.7347	0.7071
	0.25	0.7170	0.6480	0.6425	0.5524	0.5235	0.5000
	0.1	0.5422	0.4557	0.3985	0.3573	0.3336	0.3162

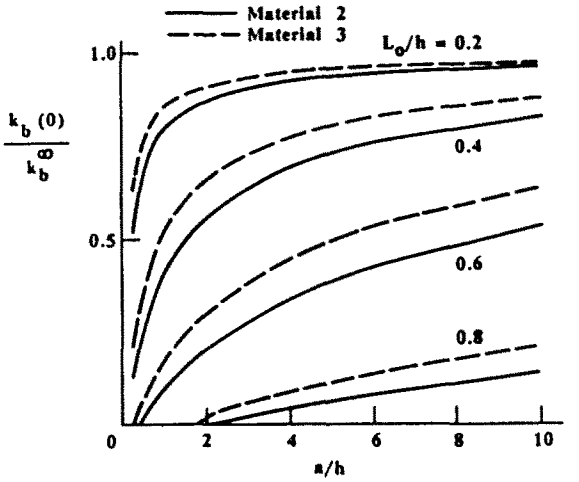

Fig. 5. The normalized stress intensity factor at the maximum penetration point of a semielliptic surface crack in an orthotropic plate under bending (Fig. 1, Table 1) (for $k_b^\infty = k_b$ see Table 3 for a corresponding crack depth $L_0 = L$).

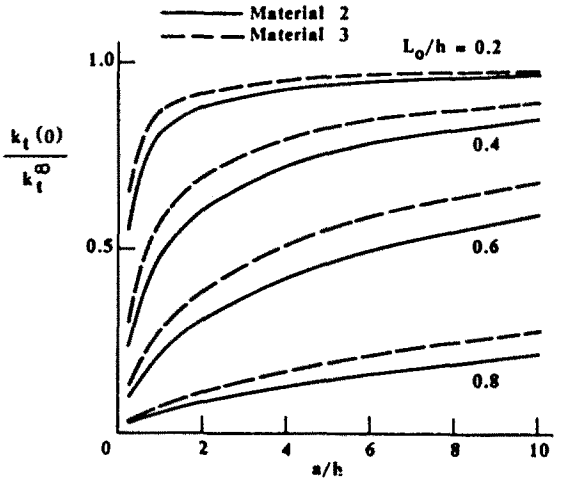

Fig. 6. The normalized stress intensity factor at the maximum penetration point of a semielliptic surface crack in an orthotropic plate under tension (Fig. 1, Tables 1 and 3).

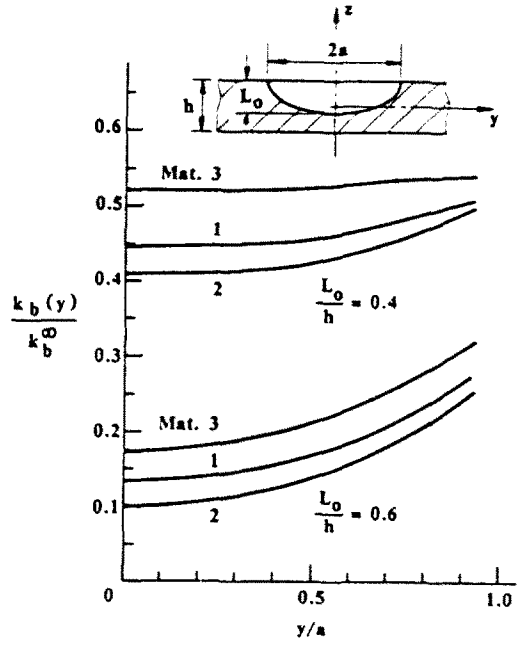

Fig. 7. The distribution of the stress intensity factor along the front of a semielliptic surface crack in a plate under bending (see Table 1 for material constants and Table 3 for K_b^∞).

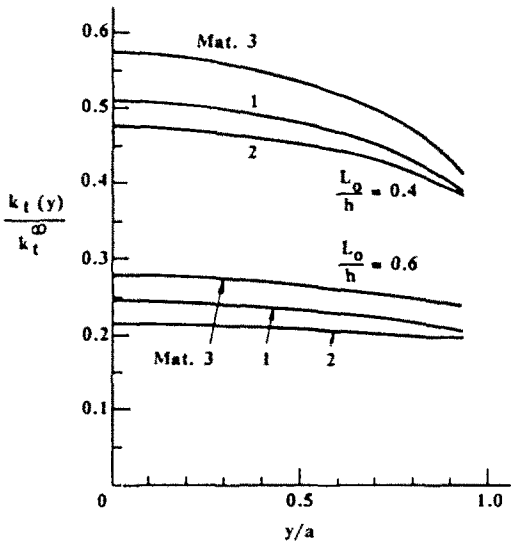

Fig. 8. The distribution of the stress intensity factor along the front of a semielliptic surface crack in a plate under tension (see Table 1 for material properties and Table 3 for K_t^∞).

stress intensity factors along the crack front in a plate under bending and tension is shown in Figs 7 and 8, respectively. These results indicate that in some cases the material orthotropy may have a significant effect on the stress intensity factors. On the other hand in a mildly orthotropic material such as TOPAZ (materials 4 and 5, see Table 2) the results for a through crack in a plate under bending is hardly distinguishable from the isotropic plate results. A similar conclusions may be drawn for a surface crack from the results given in Table 11 by comparing them with the isotropic plate solution given, e.g. by Joseph and Erdogan (1987) and Erdogan (1986).

The effect of the interaction of two coplanar semielliptic surface cracks of the same depth L_0 on the stress intensity factors in an orthotropic plate under bending and tension is shown in Tables 12–14. As expected, the interaction between surface cracks seems to be weaker than the corresponding through cracks.

Table 11. Stress intensity factor at the maximum penetration point of a semielliptic surface crack in an orthotropic plate under bending M_0 or tension N_0, materials 4 and 5. $a_1 = -a$, $b_1 = a$, $a_2 = b_2$ (Fig. 1)

Material		a/h	L_0/h 0.2	0.4	0.6	0.8
4	$\frac{k_b(0)}{k_b^\infty}$	0.5	0.710	0.303	0.049	−0.029
		1	0.809	0.441	0.130	−0.013
		2	0.872	0.575	0.233	0.015
		4	0.923	0.704	0.365	0.062
		6	0.946	0.776	0.458	0.101
	$\frac{k_t(0)}{k_t^\infty}$	0.5	0.729	0.387	0.173	0.049
		1	0.820	0.506	0.244	0.071
		2	0.881	0.623	0.332	0.102
		4	0.928	0.736	0.445	0.146
		6	0.949	0.799	0.523	0.182
5	$\frac{k_b(0)}{k_b^\infty}$	0.5	0.697	0.290	0.044	−0.0293
		1	0.797	0.424	0.121	−0.0141
		2	0.864	0.558	0.221	0.012
		4	0.918	0.691	0.351	0.057
		6	0.943	0.766	0.444	0.095
	$\frac{k_t(0)}{k_t^\infty}$	0.5	0.717	0.375	0.169	0.048
		1	0.809	0.491	0.236	0.070
		2	0.873	0.608	0.322	0.099
		4	0.923	0.725	0.433	0.142
		6	0.945	0.790	0.512	0.176
1	$\frac{k_b(0)}{k_b^\infty}$	0.25	0.585	0.184	−0.003	−0.0345
		0.5	0.715	0.309	0.053	−0.0287
		1	0.811	0.446	0.136	−0.0119
		2	0.882	0.586	0.242	0.0179
	$\frac{k_t(0)}{k_t^\infty}$	0.25	0.613	0.284	0.124	0.034
		0.5	0.733	0.392	0.176	0.050
		1	0.823	0.510	0.247	0.073
		2	0.889	0.631	0.339	0.104

Table 12. Interaction of two coplanar semielliptic surface cracks of the same depth L_0 in an orthotropic plate under bending $M_{xx}^\infty = M_0$, and tension $N_{xx}^\infty = N_0$. The stress intensity factors shown are at the maximum penetration point $L(y_i) = L_0$ of each crack: $a = (b_1 - a_1)/2$, $c = (b_2 - a_2)/2$, $d = a_2 - b_1$, $y_1 = (b_1 + a_1)/2$, $y_2 = (b_2 + a_2)/2$ (Fig. 1), $L_0/h = 0.4$, material 2

	$\frac{c}{a}$	$\frac{d}{a} \to 0.1$	0.25	0.5	1	2	∞
$\frac{k_b(y_1)}{k_b^\infty}$	1	0.444	0.437	0.430	0.423	0.417	0.409
	0.5	0.430	0.425	0.420	0.416	0.412	0.409
	0.25	0.419	0.416	0.414	0.412	0.410	0.409
	0.1	0.412	0.411	0.410	0.410	0.410	0.409
$\frac{k_b(y_2)}{k_b^\infty}$	1	0.444	1.437	0.430	0.423	0.417	0.409
	0.5	0.298	0.287	0.277	0.268	0.262	0.255
	0.25	0.171	0.158	0.148	0.140	0.135	0.130
	0.1	0.054	0.043	0.036	0.032	0.029	0.027
$\frac{k_t(y_1)}{k_t^\infty}$	1	0.505	0.500	0.494	0.488	0.483	0.477
	0.5	0.494	0.490	0.486	0.482	0.479	0.477
	0.25	0.485	0.482	0.480	0.479	0.478	0.477
	0.1	0.479	0.478	0.477	0.477	0.477	0.477
$\frac{k_t(y_2)}{k_t^\infty}$	1	0.505	0.500	0.494	0.488	0.483	0.477
	0.5	0.380	0.370	0.362	0.355	0.350	0.345
	0.25	0.270	0.250	0.252	0.245	0.241	0.237
	0.1	0.168	0.160	0.154	0.150	0.148	0.146

Finally, it should be pointed out that in plates containing through cracks or very deep part-through cracks subjected to bending only, the crack faces on the compressive side of the plate would be partially closed. Therefore, the solution given in this paper would not be valid for such problems. The solution is valid only if the plate is subjected, in addition to bending, to a membrane loading of sufficiently high magnitude so that the stress intensity

Table 13. Interaction of two coplanar semielliptic surface cracks of same depth L_0 in an orthotropic plate under bending $M_{xx}^{\infty} = M_0$, and tension $N_{xx}^{\infty} = N_0$. The stress intensity factors shown are at the maximum penetration point $L(y_i) = L_0$ of each crack: $a = (b_1 - a_1)/2$, $c = (b_2 - a_2)/2$, $d = a_2 - b_1$, $y_1 = (b_1 + a_1)/2$, $y_2 = (b_2 + a_2)/2$ (Fig. 1), $L_0/h = 0.4$, material 3

	$\frac{c}{a}$	$\frac{d}{a} \to 0.1$	0.25	0.5	1	2	∞
$\frac{k_b(y_1)}{k_b^s}$	1	0.554	0.548	0.542	0.535	0.530	0.522
	0.5	0.542	0.537	0.533	0.529	0.525	0.522
	0.25	0.532	0.529	0.527	0.524	0.523	0.522
	0.1	0.525	0.524	0.523	0.522	0.522	0.522
$\frac{k_b(y_2)}{k_b^s}$	1	0.554	0.548	0.542	0.535	0.530	0.522
	0.5	0.403	0.393	0.383	0.374	0.367	0.361
	0.25	0.256	0.242	0.231	0.223	0.217	0.212
	0.1	0.103	0.091	0.083	0.078	0.074	0.072
$\frac{k_t(y_1)}{k_t^s}$	1	0.600	0.596	0.591	0.585	0.581	0.574
	0.5	0.591	0.587	0.583	0.580	0.577	0.574
	0.25	0.582	0.580	0.578	0.576	0.575	0.574
	0.1	0.576	0.576	0.575	0.575	0.575	0.574
$\frac{k_t(y_2)}{k_t^s}$	1	0.600	0.596	0.591	0.585	0.581	0.574
	0.5	0.470	0.461	0.453	0.446	0.440	0.435
	0.25	0.343	0.332	0.324	0.316	0.312	0.308
	0.1	0.211	0.202	0.196	0.192	0.189	0.187

Table 14. Interaction of two equal semielliptic surface cracks in an isotropic and an orthotropic plate under bending M_0 and tension N_0: $a = (b_1 - a_1)/2$, $d = a_2 - b_1$, $c = a$, $a/h = 1$, $y_1 = (b_1 + a_1)/2$

Material	L_0/h	d/a 0.1	0.25	0.5	1	2	∞
				$k_b(y_1)/k_b^s$			
1	0.2	0.832	0.829	0.826	0.821	0.816	0.811
	0.4	0.488	0.481	0.470	0.465	0.456	0.446
	0.6	0.165	0.159	0.153	0.147	0.141	0.135
	0.8	−0.005	−0.006	−0.008	−0.009	−0.010	−0.011
2	0.2	0.815	0.812	0.809	0.806	0.802	0.798
	0.4	0.444	0.437	0.430	0.423	0.417	0.409
	0.6	0.121	0.115	0.110	0.105	0.101	0.097
	0.8	−0.021	−0.0224	−0.0235	−0.0245	−0.0253	−0.0260
3	0.2	0.873	0.871	0.869	0.866	0.864	0.861
	0.4	0.554	0.548	0.542	0.535	0.530	0.522
	0.6	0.201	0.194	0.189	0.183	0.178	0.172
	0.8	−0.0026	−0.0045	−0.0062	−0.0078	−0.009	−0.0103
				$k_t(y_1)/k_t^s$			
1	0.2	0.842	0.840	0.837	0.833	0.828	0.823
	0.4	0.545	0.540	0.533	0.526	0.518	0.511
	0.6	0.270	0.266	0.261	0.256	0.252	0.247
	0.8	0.076	0.076	0.075	0.074	0.073	0.073
2	0.2	0.826	0.823	0.820	0.817	0.814	0.810
	0.4	0.505	0.500	0.494	0.488	0.483	0.477
	0.6	0.234	0.230	0.226	0.222	0.219	0.215
	0.8	0.0622	0.0611	0.0602	0.0592	0.0585	0.0578
3	0.2	0.880	0.878	0.876	0.874	0.872	0.869
	0.4	0.600	0.596	0.591	0.585	0.581	0.574
	0.6	0.301	0.297	0.292	0.288	0.283	0.279
	0.8	0.0822	0.081	0.0793	0.080	0.077	0.076

factor is positive everywhere along the crack front. The problem of a plate with a through crack under pure bending is a crack-contact problem which was recently considered by Joseph and Erdogan (1989).

Acknowledgement—This work was supported by NASA Langley under Grant NAG-1-713 and by NSF under Grant MSM-8613611.

REFERENCES

Delale, F. and Erdogan, F. (1982). Application of the line-spring model to a cylindrical shell containing a circumferential or axial part-through crack. *ASME J. Appl. Mech.* **49**, 97–102.

Erdogan, F. (1978). Mixed boundary-value problems in mechanics. In *Mechanics Today* (Edited by S. Nemat-Nasser), Vol. 4, pp. 1–86. Pergamon Press, Oxford.

Erdogan, F. (1986). The line spring model. In *Computational Methods in Mechanics of Fracture* (Edited by S. N. Atluri), pp. 289–310. North-Holland, Amsterdam.

Hearmon, R. F. S. (1961). *An Introduction to Applied Anisotropic Elasticity*. Oxford University Press, Oxford.

Joseph, P. F. and Erdogan, F. (1987). Plates and shells containing a surface crack under general loading conditions. NASA Contractor Report 178328, NASA–Langley Research Center.

Joseph, P. F. and Erdogan, F. (1989). Surface crack problems in plates. *Int. J. Fracture* (in press).

Kaya, A. C. and Erdogan, F. (1980). Stress intensity factors and COD in an orthotropic strip. *Int. J. Fracture* **16**, 171–190.

Krenk, S. (1975). The stress distribution in an infinite anisotropic plate with collinear cracks. *Int. J. Solids Structures* **11**, 449–460.

Medwakowski, S. J. (1958). A refined theory of elastic orthotropic plates. *Trans. ASME J. Appl. Mech.* **25**, 437–443.

Muskhelishvili, I. N. (1953). *Singular Integral Equations*. Noordhoff, Leyden, The Netherlands.

Newman, Jr., J. C. and Raju, I. S. (1979). Analysis of surface cracks in finite plates under tension or bending loads. NASA Technical Paper 1578.

Nishioka, T. and Atluri, S. N. (1982). Analysis of surface flaw in pressure vessels by a new 3-dimensional alternating method. *J. Pressure Vessel Technol.* **104**, 299–307.

O'Donoghue, P. E., Nishioka, T. and Atluri, S. N. (1986). Analysis of interaction behavior of surface flaws in pressure vessels. *J. Pressure Vessel Technol.* **108**, 24–32.

Reissner, E. (1945). The effect of transverse shear deformation on the bending of elastic plates. *ASME J. Appl. Mech.* **12**, A69–A77.

Raju, I. S. and Newman, Jr., J. C. (1982). Stress-intensity factors for internal and external surface cracks in cylindrical vessels. *J. Pressure Vessel Technol.* **104**, 293–298.

Rice, J. R. and Levy, N. (1972). The part-through surface crack in an elastic plate. *ASME J. Appl. Mech.* **39**, 185–194.

Schäfer, V. M. (1952). Über eine verfeinerung der klassischen theorie dünner schwach gebogener platten. *Z. Angew. Math. Mech.* **32**, 161–171.

Sih, G. C. and Liebowitz, H. (1968). Mathematical theories of brittle fracture. In *Fracture an Advanced Treatise* (Edited by H. Liebowitz), Vol. 2. Academic Press, New York.

Timoshenko, S. and Woinowsky-Krieger, S. (1959). *Theory of Plates and Shells*, pp. 165–171. McGraw-Hill, New York.

APPENDIX

The functions θ_{ij} and R_j $(i, j = 1, 2, 3)$

$$\theta_{1j}(x) = \left[S_{22}m_j^2 + S_{22}A_1m_j^4 - \frac{6}{5h}(S_{22}S_{55} + S_{12}S_{44})A_1m_j^4\right]\alpha - \left[S_{22}A_2m_j^2 - S_{12} - S_{12}A_1m_j^2 - \frac{6}{5h}(S_{22}S_{55} + S_{12}S_{44})A_4m_j^2\right]x^1 - S_{12}A_2x^3 \quad \text{(A1)}$$

$$\theta_{2j}(x) = \frac{h^1}{2S_{66}}\left\{\left[\frac{1}{3}m_j + \left(\frac{1}{3}A_1 - \frac{1}{5h}S_{55}A_3\right)m_j^3 + \frac{1}{5h}S_{44}A_4m_j^5\right]x^2 - \left(\frac{1}{3}A_2 - \frac{1}{5h}S_{55}A_4\right)m_jx^4 - \frac{1}{5h}S_{44}A_1m_j^5\right\} \quad \text{(A2)}$$

$$\theta_{3j}(x) = \left[m_j + \left(A_1 - \frac{6}{5h}S_{55}A_3\right)m_j^3\right]x^2 - \left(A_2 - \frac{6}{5h}S_{55}A_4\right)m_jx^4 \quad \text{(A3)}$$

$$R_1(x) = \frac{\lambda_2 - \lambda_3}{m_1D}[\lambda_2\lambda_3Q_3 + (\lambda_3 + \lambda_2)x^2Q_4 - x^2Q_5 + x^4Q_6]\omega(x) \quad \text{(A4)}$$

$$R_2(x) = \frac{\lambda_3 - \lambda_1}{m_1D}[\lambda_3\lambda_1Q_3 + (\lambda_1 + \lambda_3)x^2Q_4 - x^2Q_5 + x^4Q_6]\omega(x) \quad \text{(A5)}$$

$$R_3(x) = \frac{\lambda_1 - \lambda_2}{m_1D}[\lambda_1\lambda_2Q_3 + (\lambda_1 + \lambda_2)x^2Q_4 - x^2Q_5 + x^4Q_6]\omega(x) \quad \text{(A6)}$$

where

$$\omega(x) = \int_L g(y)\, e^{ixy}\, dy \quad \text{(A7)}$$

$$D(\alpha) = (\alpha^4 Q_2 + \alpha^2 Q_1)[\lambda_2\lambda_3(\lambda_3-\lambda_2)+\lambda_1\lambda_3(\lambda_1-\lambda_3)+\lambda_1\lambda_2(\lambda_2-\lambda_1)] \tag{A8}$$

$$\lambda_i = m_i^2 \quad (i = 1, 2, 3) \tag{A9}$$

$$Q_1 = Q_3 = P_1P_5, \quad Q_2 = P_1(P_5P_8 - P_6P_7), \quad Q_4 = P_1P_6, \quad Q_5 = P_2P_5, \quad Q_6 = P_3P_6 - P_4P_5 \tag{A10}$$

$$P_1 = \frac{h^5 S_{44}S_{22}}{120\Delta S_{66}}, \quad P_2 = \frac{h^3}{6S_{66}}, \quad P_3 = -\frac{h^3}{120\Delta S_{66}}(S_{22}S_{55}+S_{12}S_{44})$$

$$P_4 = \frac{h^5 S_{55}S_{12}}{120\Delta S_{66}}, \quad P_5 = \frac{h^3 S_{22}}{12\Delta}, \quad P_6 = \frac{h^3 S_{12}}{12\Delta} - \frac{h^3}{6S_{66}}$$

$$P_7 = \frac{h^2 S_{44}}{10S_{66}} - \frac{h^2 S_{12}S_{44}}{10\Delta}, \quad P_8 = \frac{h^2 S_{55}S_{12}}{10\Delta} - \frac{h^2 S_{55}}{10S_{66}} \tag{A11}$$

$$\Delta = S_{11}S_{22} - S_{12}S_{21}. \tag{A12}$$